

This work was written as part of one of the author's official duties as an Employee of the United States Government and is therefore a work of the United States Government. In accordance with 17 U.S.C. 105, no copyright protection is available for such works under U.S. Law.

Public Domain Mark 1.0

<https://creativecommons.org/publicdomain/mark/1.0/>

Access to this work was provided by the University of Maryland, Baltimore County (UMBC) ScholarWorks@UMBC digital repository on the Maryland Shared Open Access (MD-SOAR) platform.

Please provide feedback

Please support the ScholarWorks@UMBC repository by emailing scholarworks-group@umbc.edu and telling us what having access to this work means to you and why it's important to you. Thank you.



Development of an End-to-End Demonstration Readout Chain for Athena/X-IFU

S. Beaumont^{1,2,3}  · F. Pajot¹ · G. Roudil¹ · J. S. Adams^{2,3} · S. R. Bandler² · B. Bertrand¹ · G. Betancourt-Martinez¹ · F. Castellani¹ · J. A. Chervenak² · C. Daniel⁴ · E. V. Denison⁵ · W. B. Doriese⁵ · M. Dupieux¹ · M. Durkin⁵ · H. Geoffroy⁴ · G. C. Hilton⁵ · Y. Parot¹ · P. Peille⁴ · D. Prêle⁶ · L. Ravera¹ · C. D. Reintsema⁵ · K. Sakai^{2,3} · S. J. Smith² · R. W. Stevens⁵ · J. N. Ullom⁵ · L. R. Vale⁵ · N. A. Wakeham^{2,3}

Received: 2 November 2021 / Accepted: 17 June 2022

© The Author(s), under exclusive licence to Springer Science+Business Media, LLC, part of Springer Nature 2022

Abstract

The X-ray Integral Field Unit (X-IFU) of the Athena observatory, scheduled for launch in the mid 2030's, will provide X-ray spectroscopy data with unprecedented spectral and spatial resolution. This will be achieved with a 2 kilo-pixel array of transition-edge sensor (TES) microcalorimeters. The complete detection chain is under development by a large international collaboration. In order to perform an end-to-end demonstration of the X-IFU readout chain, a 50 mK test bench is being developed at IRAP in collaboration with CNES. The test bench uses a two-stage ADR cryostat from Entropy GmbH, a 1024-pixel array, and will initially be operated using a warm electronics chain from NIST and NASA Goddard Space Flight Center. We describe the complete system being installed in the cryostat and the current results obtained with these electronics. We also review the status of the integration of the digital readout electronics (DRE) prototype into the demonstration chain and the plan for integrating and testing the complete X-IFU readout chain.

Keywords X-ray instrumentation · Athena/X-IFU · End-to-end readout

✉ S. Beaumont
sophie.beaumont@nasa.gov

¹ IRAP, CNRS, Université de Toulouse, UPS, Toulouse, France

² NASA GSFC, Greenbelt, USA

³ CRESST II – UMBC, Baltimore, USA

⁴ CNES, Paris, France

⁵ NIST-Boulder, Boulder, USA

⁶ APC, CNRS, Université de Paris, Paris, France

1 Introduction

The Advanced Telescope for High-ENergy Astrophysics (Athena) [1], scheduled for launch in the mid 2030's, will revolutionize X-ray astrophysics. This ESA large class mission will address the science theme of the Hot and Energetic Universe, trying to answer key questions such as how ordinary matter assembles into the large-scale structures we see today, and how black holes grow and shape the Universe. It will consist of a single X-ray telescope associated with two instruments: a wide field imager (WFI) and an X-ray integral field unit (X-IFU). The X-IFU [2], a cryogenic imaging spectrometer operating at 55 mK, will provide spectral data with unprecedented performance, with a full-width-at-half-maximum energy resolution of 2.5 eV for energies up to 7 keV – a factor~50 better than CCDs. This will be achieved using close to 2,400 transition edge sensor (TES) microcalorimeters, optimized for the soft X-ray energy band (0.2 – 12 keV), with a pixel size of 5 arc-seconds and a field-of-view of 5 arc-minutes. It will have a count rate capability for point sources (using the defocus capability of the telescope) of up to 10 mCrab with nominal resolution, and 1 Crab with 10 eV resolution and a Be filter.

To limit the mass, power, heat load and complexity of the instrument it is necessary to multiplex the read-out of the detector array, which will be achieved using time division multiplexing (TDM) [3]. In this scheme, the TESs which are DC voltage-biased using a shunt resistor are individually inductively coupled to one of the front-end SQUIDs (superconducting quantum interference devices) (also referred to as SQ1 or MUX SQUIDs). Those SQUIDs are turned on/off sequentially using switches to measure the signal from each of the TESs multiplexed together in each row. As the number of elements per column is limited to meet the instrument capabilities and requirements (for X-IFU to 34 rows), this can be replicated as many times as needed, by having multiple columns read out in parallel, independently from one another. For each column, the multiplexed output from the front-end SQUIDs is then amplified by the second stage series array amplifier SQUIDs (AMP SQUIDs), and a low noise amplifier at room temperature. To keep the SQUIDs in a linear and stable regime of operation, the system is run in a closed loop (fluxed-lock loop). A simplified circuit diagram describing the above can be found in Fig. 1.

For the X-IFU, the read-out chain will be integrated under a collaboration of 11 European countries, the USA and Japan, led by IRAP and CNES (France). Each component of the system is currently being developed separately, summarized in Table 1.

For the success of the mission, it is hence crucial that the full baseline detection chain, from the TES detectors at 50 mK to the warm electronics at room temperature, is successfully integrated and tested. To do this, IRAP and CNES have been developing a 50 mK test bench for demonstrating prototypes of all these flight-like components functioning together, and to understand the performance of the whole detection chain through a comparison with an advanced model that is a very detailed end-to-end simulator of the entire detection chain [4]. It will provide valuable feedback for the development of the warm readout electronics and will later be used to characterize the X-ray calibration sources.

Fig. 1 Circuit diagram of a TDM system for 1 column and 2 rows (based on [3]). Min and Mfb are the mutual inductances of the SQ1 input and feedback coils; Lny the Nyquist inductance; Rsh_tes and Rsh_sq the TES and SQ1 shunt resistances; RA the row addressing; and FB the part of the electronics handling the fluxed-lock loop

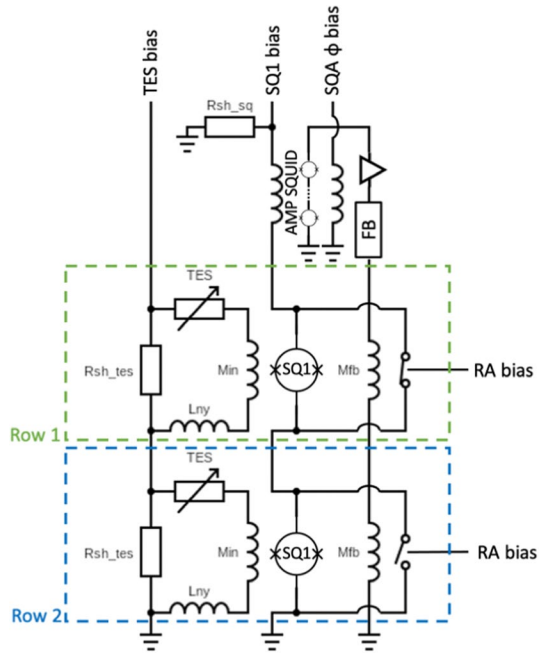


Table 1 Summary of the components of the detection chain and of the institutions where they are being developed

Components	Institution
Detector array [5]	NASA GSFC (U.S)
Cold time domain multiplexing (TDM) electronics [6]	NIST (U.S)
Cold amplifier [7]	VTT (Finland)
Cold focal-plane assembly (FPA) [8]	SRON (Netherlands)
Warm front-end electronics (WFEE) [9]	APC (France)
Digital readout electronics (DRE) [10], including:	IRAP (France), with:
Hardware part of the Event processor	CEA (France)
Software part of the Event processor	INTA (Spain)
Demux boards	ASU (Czech Republic)

2 IRAP/CNES 50 mK Test Bench

The test bench includes a commercial cryostat purchased from Entropy GmbH (Fig. 2). It consists of a 2-stage pulse tube cryocooler (PTR), which provides cooling to 50 K and 3 K, and of a 2-stage adiabatic demagnetization refrigerator (ADR) to provide cooling at 500 mK (with a gadolinium gallium garnet (GGG) salt pill) and at 50 mK (with a ferric aluminum alum (FAA) salt pill).

A full characterization of the cryostat has been performed prior to integration of the various subsystems from the X-IFU detection chain. This included a study of the

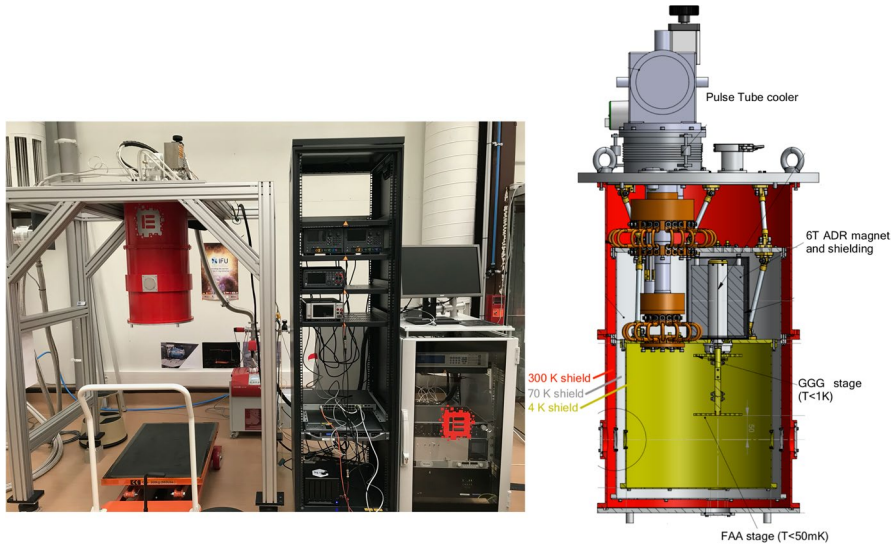


Fig. 2 (left) 50 mK test cryostat (nicknamed “Elsa”) and its current electronics at IRAP (right) Schematic of the cryostat

magnetic environment, an assessment of the micro-vibrations, and a characterization of the temperature stability, hold time, and heat loads at 55 mK. This was necessary to ensure that the TES detectors and SQUID-based read-out are operated under suitable conditions for optimal performance. Both are highly sensitive to magnetic fields (both static and dynamic), and the detectors are highly sensitive to temperature fluctuations of the thermal bath. A summary of this characterization is given below. Further details can be found in the SPIE proceedings from Betancourt-Martinez et al. [11].

The temperature stability and hold time were studied using a Lakeshore 372 AC resistance bridge, and Cernox thermistors for the 0.5 K, 3 K and 50 K stages, and a RuO_2 thermistor for the 50 mK stage. This showed a $3 \mu\text{K}$ rms temperature stability—within our requirements for this test bench—, and 11 h of hold time at 55 mK with an additional $0.5 \mu\text{W}$ heat load on the FAA stage. This is well above the expected load for our FPA, estimated to be around 14 nW maximum.

The magnetic field environment was studied using a Bartington Mag-01H Single Axis Fluxgate Magnetometer, together with cryogenic Probes F & G (with, respectively, 0.1 nT and 1 nT resolution). This showed a $1.4 \mu\text{T}$ (total) static residual B-field due to the earth’s magnetic field shielded with an external mu-metal external shield, and a less than 25 nT/15 min B-field slew rate during ADR regulation at the location of the array (without consideration of the expected attenuation from a superconducting shield around the detector set-up, which is expected to be around 2000 or more).

Finally, the micro-vibrations were assessed using PCB piezotronics accelerometers (two 393B04’s with $3 \mu\text{g}$ rms broadband sensitivity, and one 351B42 working at cryogenic temperatures). This gave levels of 6.50 mg rms, 2.37 mg rms and

0.099 mg rms, respectively, over the 0–100 Hz, 100–1600 Hz and 1600–5000 Hz frequency bands. Those results were similar to measurements made at SRON [12] and known to be acceptable.

3 Read-Out Chain for Initial Validation

Following the characterization of the 50 mK test bench, we will soon begin integrating sub-systems (see high level diagram on Fig. 3). The initial system validation is to be carried out first using non-flight electronics from NIST and GSFC with the heritage of having demonstrated the required performance.

We will use analog low noise amplifiers at room temperature provided by NIST with a noise level of less than $1 \text{ nV}/\sqrt{\text{Hz}}$ [6], which perform the same function as will be provided by the X-IFU WFEE [9]. The analog electronics box ('tower') also provides bias currents for the front-end multiplexed SQUIDs and the second stage AMP SQUIDs.

For the TDM multiplexing, we will be using digital electronics provided by GSFC that is based upon commercial off-the-shelf (COTS) electronics boards [13]. These will perform a similar function to the X-IFU flight DRE to be provided by IRAP [10], providing column selection and row switching (with timing signals) for TDM.

The read-out chain also consists of harnesses and cold electronics. This starts with flex wiring fabricated from Cu-Ni traces on Kapton flex going from 300 to

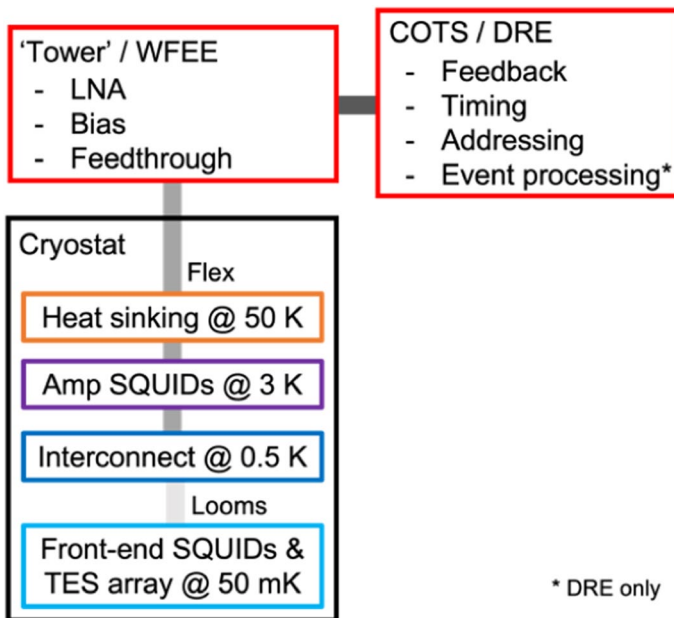
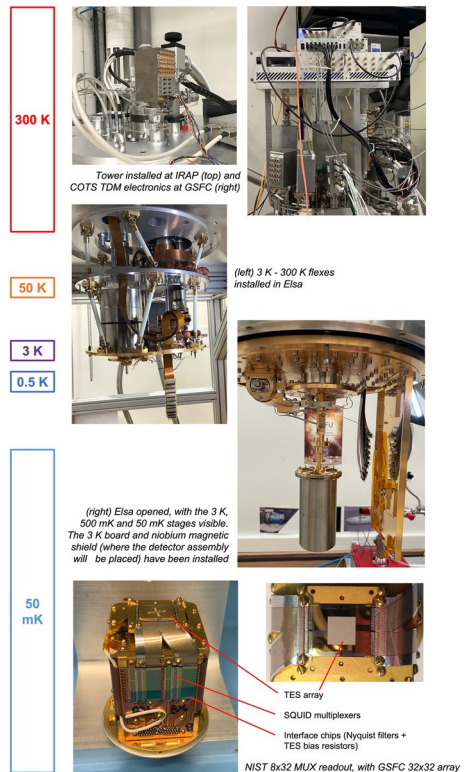


Fig. 3 High level diagram of the read-out demonstration chain

Fig. 4 Breakout view of the subsystems from the initial E2E demonstration chain



3 K, which passes through an epoxy hermetic feedthrough and is heat-sunk at 50 K before being terminated at the 3 K stage. The signal wiring is connected to the second stage AMP SQUID amplifiers at 3 K which are provided by NIST.

The input signals to the AMP SQUIDs as well as those that run directly to the low-temperature multiplexer are carried on superconducting twisted pairs in looms that are heat-sunk at a 500 mK interconnect board (provided by GSFC), before the signals pass through to the 50 mK stage.

Finally at the end of the read-out chain, at the 50 mK stage, are the TES detectors provided by NASA-Goddard [5]. These are coupled to the cold multiplexer read-out electronics provided by NIST that perform switch addressing and hold the front-end SQUIDs [6]. The 50 mK test bench can accommodate a 32×32 TES microcalorimeter array (absorber pitch of $275 \mu\text{m}$ and TESs with dimensions $75 \times 75 \mu\text{m}$). For this demonstration chain, it was decided for simplicity and efficiency initially to populate and connect only two columns of the read-out out of a possible eight available, providing a 2×32 demonstration system. Pictures of the various parts of the read-out chain are shown in Fig. 4.

4 First Results and Way Forward

4.1 Initial Results

The ‘snout’ (TES detectors + cold read-out electronics) has been tested at NASA-Goddard together with the same warm readout electronics described in Sect. 2 and these have been sent to IRAP for integration. Single pixel measurements showed good uniformity and an energy resolution of 2.1 ± 0.1 eV at 6 keV as shown in Fig. 5. Multiplexed measurements, using 2×32 pixels, also showed a preliminary energy resolution of 2.63 ± 0.01 eV. It should be pointed out however that although adequate for initial demonstration, this level of performance is not (and was not meant to be) the ultimate optimized multiplexed performance achievable for these detectors [5].

4.2 Installation at IRAP

As of mid-October 2021, the flexes and analog electronics have been installed on the test bench. The focal plane assembly ‘snout’ and COTS TDM electronics have been received as well by IRAP and are scheduled for integration imminently. This will be followed by mechanical alignment checks at 3 K. The full initial demonstration chain will then be tested at IRAP for validation, to be ready for the DRE TDM row addressing tests later in the fall of 2021.

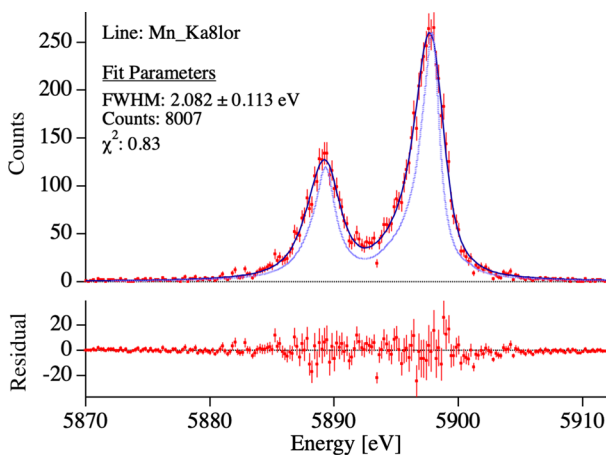


Fig. 5 Example of single pixel spectrum measured at NASA-Goddard with the focal plane assembly that has been shipped to integrate with the rest of the test-bench at IRAP

4.3 DRE Prototype Integration Status

The Demonstration Model (DM) of the DRE will be tested in several steps in the 50 mK test bench. This fall, the Row Address and Synchronization (RAS) module (driving the Flux Actuated Switches in the focal plane assembly (FPA) and synchronizing the readout electronics) will be tested together with the U.S. digital electronics. Beginning 2022, a 4-column DEMUX module will also be implemented in the set-up. This module demultiplexes the pixel's data and linearizes the detection chains. The digital signal event processing (triggering of the events and measurement of the energies) will be done in software using a computer from the test bench. By mid 2022, a test is planned with a prototype of the flight event processor to validate its high-speed interface with the DEMUX module. Finally, at the end of 2022, a demonstrator of the DRE DC-converter will be coupled to the other modules.

4.4 Integration and Testing of the Complete X-IFU Readout Chain

The full end-to-end demonstration with the WFEE is scheduled for end 2022. Aiming at reaching the best possible noise level, the WFEE is being developed using differential electronics, while the current chain based on legacy electronics is single-ended. The 3 K AMP SQUID board and the cold harness from 3 to 300 K will hence also need to be updated to support differential electronics. Procedures for the various flight operation modes for all the electronics will then be tested.

Acknowledgements Part of the material presented is based upon work supported by NASA under award number 80GSFC21M0002.

References

1. Nandra et al., 2013, Athena white paper
2. Barret et al., 2018, Proceedings SPIE, Vol. 10699, 106991G
3. Durkin et al., 2019, IEEE TAS, Vol. 29, no. 5, 2101005
4. Lorenz et al., 2020, J Low Temp Phys, Vol. 200, p.277
5. Smith et al., 2021, IEEE TAS, Vol. 31, no. 5, 2100806
6. Doriese et al., 2016, JLTP, Vol. 184, p.389
7. Kiviranta et al., 2021, IEEE TAS, Vol. 31, no. 5, 9357957
8. Geoffray et al., 2020, Proceedings SPIE, Vol. 11444, 114440X
9. Chen et al., 2018, Proceedings SPIE, Vol. 10699, 106994P
10. Ravera et al., 2018, Proceedings SPIE, Vol. 10699, 106994V
11. Betancourt-Martinez et al., 2021, Proceedings SPIE, Vol. 11444, 1144401
12. SRON, private correspondence
13. Sakai et al., 2021, J Low Temp Phys, This Special Issue

Publisher's Note Springer Nature remains neutral with regard to jurisdictional claims in published maps and institutional affiliations.

Springer Nature or its licensor holds exclusive rights to this article under a publishing agreement with the author(s) or other rightsholder(s); author self-archiving of the accepted manuscript version of this article is solely governed by the terms of such publishing agreement and applicable law.